AoB PLANTS
The open-access journal for plant sciences

Research Article

Root hydraulic conductivity and adjustments in stomatal conductance: hydraulic strategy in response to salt stress in a halotolerant species

Victoria Vitali[1], Jorge Bellati[1], Gabriela Soto[2], Nicolás D. Ayub[2] and Gabriela Amodeo[1]*

[1] Departamento de Biodiversidad y Biología Experimental, Facultad de Ciencias Exactas y Naturales, Instituto de Biodiversidad y Biología Experimental, Universidad de Buenos Aires and Consejo Nacional de Investigaciones Científicas y Técnicas, C1428EGA Buenos Aires, Argentina

[2] Instituto de Genética "Ewald A. Favret", CICVyA, INTA-Castelar and Consejo Nacional de Investigaciones Científicas y Técnicas, 1686 Buenos Aires, Argentina

Received: 2 April 2015; **Accepted:** 7 November 2015; **Published:** 24 November 2015

Associate Editor: Tim J. Brodribb

Citation: Vitali V, Bellati J, Soto G, Ayub ND, Amodeo G. 2015. Root hydraulic conductivity and adjustments in stomatal conductance: hydraulic strategy in response to salt stress in a halotolerant species. *AoB PLANTS* **7**: plv136; doi:10.1093/aobpla/plv136

Abstract. Recent advances at the molecular level are introducing a new scenario that needs to be integrated into the analysis of plant hydraulic properties. Although it is not yet clear to what extent this scenario alters the current proposal for the hydraulic circuit models, it introduces new insights when studying plants that are able to easily overcome water restrictions. In this context, our aim was to explore water adjustments in a halotolerant model (*Beta vulgaris*) by studying the coordination between the root in terms of root hydraulic conductivity (L_{pr}) and the shoot as reflected in the stomatal conductance (g_s). The root water pathways were also analysed in terms of root suberization (apoplastic barrier) and aquaporin transcript levels (cell-to-cell pathway). *Beta vulgaris* showed the ability to rapidly lose (4 h) and gain (24 h) turgor when submitted to salt stress (200 mM). The reduction profile observed in L_{pr} and g_s was consistent with a coupled process. The tuning of the root water flow involved small variations in the studied aquaporin's transcripts before anatomical modifications occurred. Exploring L_{pr} enhancement after halting the stress contributed to show not only a different profile in restoring L_{pr} but also the capacity to uncouple L_{pr} from g_s. *Beta vulgaris* root plays a key role and can anticipate water loss before the aerial water status is affected.

Keywords: Aquaporins; *Beta vulgaris*; root hydraulic conductivity; salt stress; soil–plant–atmosphere continuum; stomatal conductance; suberization; water relations.

Introduction

Water flow through plants has been described as a passive mechanism (diffusion and bulk flow) based on the analogy with Ohm's law (Van den Honert 1948). The movement of water along a hydraulic circuit with resistances (R, m^{-3} s MPa) to the water flow at the root, shoot and canopy levels is known as the soil–plant–atmosphere continuum or SPAC (Tardieu and Davies 1993; Suku *et al.* 2014). Given a water potential gradient ($\Delta\Psi$, MPa), an increase or decrease in the water flow (J_v, $m^{-3}\ s^{-1}$) will reflect a change in the hydraulic conductance (L_o, $m^3\ s^{-1}\ MPa^{-1}$) along the plant's hydraulic circuit. In this model, the daytime transpiration demand of the aerial part of the plant—modulated by stomatal

* Corresponding author's e-mail address: amodeo@bg.fcen.uba.ar

conductance (g_s, mmol m^{-2} s^{-1})—is the main contributor to the driving force that ensures water entry through the roots (Sack and Holbrook 2006).

Thus, hydraulic integration can be considered to be a trait with important implications for plant structure and function (Schenk *et al.* 2008). In the last decade, considerable attention has been given to discover how root hydraulic properties affect the overall water uptake. Despite analysing changes in the absorbing surface area or modifications in the driving force, a new approach is provided that considers the intrinsic water uptake properties of the root (hydraulic conductivity, L_{pr}) as a key component of the capacity to transport water per unit surface and per driving force (Steudle and Peterson 1998; Steudle 2000; Tyree 2003). The discovery of aquaporins has contributed to a reconsideration of the paradigm of the membrane transport capacity in terms of water and/or certain solutes or gases (Maurel 1997; Javot and Maurel 2002; Tyerman *et al.* 2002; Hachez and Chaumont 2010; Alleva *et al.* 2012; Chaumont and Tyerman 2014). According to the 'composite transport model' (Steudle 2000), the magnitude of the osmotic and hydrostatic forces will determine which path is the primary contributor to water flow: the apoplastic pathway (with low resistance) and/or the cell-to-cell pathway (i.e. symplastic plus transcellular, with high resistance) (Steudle and Peterson 1998; Suku *et al.* 2014). However, it is not only a question of how limiting the radial water flow could be but also to what extent these two pathways can be modified to rapidly adjust the L_{pr}. Recent findings emphasize that aquaporins might substantially contribute to water uptake (e.g. barley: Knipfer and Fricke 2011; soybean: Vandeleur *et al.* 2014). Evidence for the contribution of the radial water flow has been identified by applying hydrostatic pressure to the root medium (Boursiac *et al.* 2005; Hachez *et al.* 2012; Vandeleur *et al.* 2014) or by dissecting the hydrostatic and osmotic gradients in the entire plant (Fritz *et al.* 2010; Fricke *et al.* 2013; Gambetta *et al.* 2013).

The impact of the radial water flow on the hydraulic circuit could be analysed by studying the response of plants in conditions where the hydraulic driving force limits water absorption. For instance, salt stress is a condition in which both the excessive Na^+ in the soil environment and the water deficit act as linked factors that severely affect the plant growth rate. High salt concentration reduces soil water potential and not only makes water absorption harder for the roots but also introduces toxicity through a gradual accumulation of ions in the plant tissues (Munns and Tester 2008). Thus, the fine regulation between the ion redistribution and the water flow pathways is crucial in the tolerance response. The relevance of membrane pathways involved in ion redistribution—particularly between Na^+ and K^+—has been well described (Niu *et al.* 1995; Peng *et al.* 2004; Karley and White 2009; Shabala *et al.* 2010; Gajdanowicz *et al.* 2011). It is still necessary to understand how water pathway resistances (or conductances) contribute to improve plant salt tolerance.

Beta vulgaris—a member of the Chenopodiaceaea family—is considered a halotolerant (Clarke *et al.* 1993) or moderately salt-tolerant glycophyte (Bartels and Sunkar 2005; Bartels and Dinakar 2013). This behaviour among beet subspecies is related to their versatile ability to accomplish a rapid osmotic adjustment by regulating their ion and water uptake (Daoud *et al.* 2008). In these plants, the decrease in the water potential imposed by salinity is overcome by osmotic regulatory mechanisms, and the plants gain the capacity to take up water from the saline medium and maintain their turgor. An isolated enriched fraction of *B. vulgaris* plasma membrane shows very high water permeability ($P_f = 542$ μm s^{-1}; Alleva *et al.* 2006) that favours a highly permeable cell-to-cell pathway. To date, three *B. vulgaris* plasma membrane intrinsic proteins (*Bv*PIP1;1, *Bv*PIP2;1 and *Bv*PIP2;2) have been described (Qi *et al.* 1995; Barone *et al.* 1997, 1998) and characterized in a heterologous system (Bellati *et al.* 2010; Jozefkowicz *et al.* 2013). Because the *B. vulgaris* genome was very recently announced (Dohm *et al.* 2014), transcriptome global sequencing (Mutasa-Göttgens *et al.* 2012) as well as expressed sequence tag libraries provide excellent sources for open reading frame identification for tissue and/or different growth conditions (http://compbio.dfci.harvard.edu). The latter sources are precise enough to provide confidence that, to date, the three identified *Bv*PIPs described in this work remain the consistently abundant and highly expressed ones (Skorupa-Kłaput *et al.* 2015).

In an environmental condition with low water availability in the soil, the root water pathways can combine anatomical/architectural changes with the adjustment of aquaporin contribution, which might finally be reflected in the L_{pr} (Hachez *et al.* 2006; Maurel *et al.* 2010; Chaumont and Tyerman 2014). In particular, plants under salt stress might decrease L_{pr} by means of different strategies, including (i) the modulation of aquaporin by post-transductional mechanisms (Boursiac *et al.* 2005, 2008; Luu *et al.* 2012) or by transcriptional changes (Jang *et al.* 2004; Mahdieh *et al.* 2008; Horie *et al.* 2011; Muries *et al.* 2011; Liu *et al.* 2012) and (ii) changes in the root architectural arrangement (Galvan-Ampudia and Testerink 2011; Horie *et al.* 2012) and/or anatomical changes (Bramley *et al.* 2009), including suberin deposition (Krishnamurthy *et al.* 2011; Sutka *et al.* 2011). Thus far, the above-mentioned mechanisms described in (i) are associated with faster and reversible responses (hours–days), while those described in (ii) are related to long and irreversible acclimation triggered days after the onset of the stress (Munns and Tester 2008; Horie *et al.* 2012).

The aim of this work was to explore how hydraulic adjustments improve the tolerance response in a halotolerant species by analysing L_{pr} and g_s changes. The dynamics of root water adjustment (including water pathways) was explored under two salt treatments (200 mM NaCl and 200 mM KCl). Sodium ion was replaced with K^+ to provide a source of a different monovalent cation as an inorganic osmolyte (Rahnama *et al.* 2010). This experimental design (NaCl versus KCl) was introduced because the ion redistribution is different, i.e. Na^+ linked to the apoplast versus K^+ linked to the transcellular pathway (Tester and Davenport 2003; Shabala and Cuin 2008). These redistributions will affect not only the water fluxes but also the water pathways involved. Our working hypothesis is that changes in resistances (or conductances) should also be accomplished to rapidly adjust the plant hydraulics. Although ABA and signalling crosstalk have been extensively addressed in the literature (Finkelstein 2013; Geng *et al.* 2013; Mittler and Blumwald 2015), the contribution of our work is to analyse in detail the hydraulic continuum associated with tolerance by performing a biophysical study to quantify the water adjustments.

To achieve this goal, our experimental design (NaCl versus KCl salt treatment) included (i) exploration of the plant hydraulic dynamics analysing two conditions that reflect different root–shoot water status in *B. vulgaris* (loss of turgor and gain of turgor) after being submitted to salt treatments and (ii) exploration of the hydraulic adjustment capacity to recover after the salt treatment is halted, thus assessing the contribution of the water pathways. We analysed physiological parameters linked to the water adjustment capacity at the whole-plant level: water potential, g_s and L_{pr}, together with the amount of *Bv*PIPs aquaporin's transcripts and root anatomical modifications. Our hypothesis is that the tolerance of *B. vulgaris* to salt stress may be explained in terms of a high capacity to perform hydraulic adjustments and that this capacity might quantitatively reflect root plasticity that functions as a rheostat in the SPAC (Maurel *et al.* 2010).

Methods

Characterization of a new state for *B. vulgaris* under salt stress

Plant growth and experimental design. *Beta vulgaris* was grown under controlled environmental conditions with a 16/8 h light/dark cycle in a 21 °C conditioned growth chamber (light intensity conditions were 148 ± 10 μmol m^{-2} s^{-1}). Red beet seeds were germinated in plastic containers filled with sterilized sand and moistened with hydroponic culture: 1.25 mM KNO_3, 0.75 mM $MgSO_4$, 1.5 mM $Ca(NO_3)_2$, 0.5 mM KH_2PO_4, 50 μM FeEDTA, 50 μM H_3BO_3, 12 μM $MnSO_4$, 0.70 μM $CuSO_4$, 1 μM $ZnSO_4$, 0.24 μM Na_2MoO_4 and 100 μM Na_2SiO_3 (Javot *et al.* 2003). Ten days after germination, the healthy seedlings were transplanted into aerated hydroponic culture containers. Distilled water was added on the 10th day to compensate for the losses by evapotranspiration. For all of the studied parameters, a nutrient solution was complemented or not with NaCl or KCl (200 mM) at 21 days after planting, i.e. when the first true leaf was completely mature. The treatments were always started at the beginning of the light cycle (9:00 AM), which was considered to be time 0 h. The subsequent harvest time(s), where any parameter was measured and/or samples taken, are in reference to this initial ($t = 0$ h) time. All treatments were applied in a completely randomized design. At least three to four independent biological replicates were used in each experiment. Data are expressed as the mean of three performed independent experiments. The final salt concentration was selected by analysing the plant's response to different NaCl treatments (50, 100, 250 and 500 mM) **[see Supporting Information—Fig. S1]**. Our strategy was to find a physiological condition where hydroponically grown plants were able to rapidly show a clear change in their phenotype (loss of turgor), followed by a gain of turgor after the onset of salt stress. This phenotype change was remarkable at 200 mM NaCl ($\Psi_{medium} = -0.90$ MPa).

Relative water content. The first true leaf was collected from different plants at different time intervals after treatment and employed to determine relative water content (RWC), as described by Turner (1981). The turgid weight was measured on the same leaves after immersing them for 24 h (until the final weight value was constant) in distilled water, and the oven-dry weight (DW) was obtained after drying them at 70 °C for 24 h (until the final weight value was constant).

Transpiration rate. The volume of water transpired per plant was measured gravimetrically. The plants were grown as follows: 1 day before the treatment was applied, each plant was moved to an individual plastic container, which was sealed to prevent evaporation. Every plant was weighed every hour between 9:00 AM and 5:00 PM during four consecutive days. In each plant, the slope of mass = f(time) was employed to calculate the average mass lost per hour per leaf area per day for all treatments (6–9 plants). In all cases, we determined the leaf area only on the fourth day, and this value was used to calculate the transpiration rate.

Relative growth rate of leaf area. The leaf blades (first true leaf) of the plants were photographed with a digital camera, and the leaf area was measured with image analysis software (Image J ver. 1.37; http://rsb.info.

nih.gov/ij). The relative growth rate (RGR) was calculated with respect to the ratio of A_i (leaf area in a given time) and A_o (leaf area at the beginning of experiment), and the results were expressed as the natural logarithm of the relative leaf area (A_i/A_o) as a function of time (from $t = 0$ h—onset of the salt treatment—up to 48 h). The slope of the curve estimates RGR.

Shoot–root ratio. To analyse the biomass distribution, the shoot–root ratio was determined from the fresh weight in each experimental condition (control, 200 mM NaCl, 200 mM KCl at 0, 4, 8, 24 and 48 h of the imposed treatment).

Apparent leaf water potential. The leaves of the treated or control plants were placed in a plastic bag covered with Parafilm® foil prior to measurement in a Scholander pressure chamber (BioControl, Model 4, Argentina) to determine Ψ_{leaf} (Scholander *et al.* 1965). The measured leaf water potential in this work is referred to as the apparent leaf water potential (Ψ'_{leaf}) because in species such as *B. vulgaris*—which shows halotolerant features—the osmotic potential (Ψ_{osm}) of the xylem is not negligible (Boyer 1969; Kaplan and Gale 1974). It is, therefore, considered as an estimator of the water potential (Turner 1981).

Apparent turgor-pressure component. The pressure component of the water potential (Ψ'_p) in the leaf was calculated as $\Psi'_p = \Psi'_{leaf} - \Psi_{osm}$. In another set of leaves, we determined the Ψ_{osm} following a freezing protocol as previously described (Mahdieh *et al.* 2008). The osmolality of each sample was measured in a vapour pressure osmometer (Vapro 5520, Wescor, USA) **[see Supporting Information—Table S1]**.

Linking root hydraulic response to the overall SPAC

Stomatal conductance measurements. Stomatal conductance was measured with a steady-state porometer (SC-1, Decagon Devices, Pullman, WA, USA) on the first true leaf in each plant, a completely expanded mature one. To avoid time-consuming measurements, we first demonstrated that the measurement of one leaf was sufficient per plant, i.e. the g_s profile was similar between leaves in each plant during the day (data not shown).

Root hydraulic conductivity measurement. Measurements were performed as previously described (Javot *et al.* 2003; Boursiac *et al.* 2005). In these experiments, the entire root system of a freshly detopped plant was inserted into a 50-mL tube filled with the same nutrient solution bathing the intact plant, and the root was then placed inside the pressure chamber (BioControl, Model 2, Argentina). The hypocotyl was carefully connected to a glass capillary tube using a low-viscosity dental paste (A+ Silicone, Densell) and was then threaded through the metal lid of the chamber. We determined the exudated flow (J_v) induced by the pressure. Briefly, the excised roots were subjected to three pressures in a stepwise manner: 0.3, 0.4 and 0.2 MPa. The exudated flow was constant in all time periods of measurement (5–10 min in each pressure). After measurements, the DW of the root was obtained. The L_{pr} of each individual root system (in mL mg^{-1} h^{-1} MPa^{-1}) was calculated from the slope of a plot of flow (J_v) versus pressure divided by the DW of the root system **[see Supporting Information—Graph S1]**. Diurnal effects were discarded measuring both properties during the day in control plants. The change in treated plants was statistically significant and independent of the time of the day.

Exploring root adjustments in terms of water pathways

Root anatomy. As described by Sharp *et al.* (2004), roots were cut in an equivalent position with respect to both root meristem and whole root length to warranty identical ontogenetic state for all the treatments. Fresh roots were cut into pieces 10 mm in length and incubated in 0.3 % w/v Sudan IV (Sigma-Aldrich) (in ethanol 70 %, v/v) for 1 h (Sutka *et al.* 2011). The root fragments were then rinsed in distilled water and finely chopped using a razor blade. The samples were mounted on slides in glycerol and observed with a microscope (Zeiss Axioskop 2, Japan). We found a better pattern for the Sudan IV red-stained root with respect to autofluorescence in the free-hand cross-sections, and measurements of L_{pr} can be made in the same sample without fixing the material.

Quantitative real-time polymerase chain reaction for aquaporin gene expression

The roots were carefully and quickly harvested, frozen in liquid nitrogen and stored at −70 °C. The total RNA was isolated from 70 to 80 mg of tissue using 'RNeasy Plant Extraction kit' with 'Plant RNA Isolation Aid' (Ambion, Austin, TX, USA) according to the manufacturer's recommendation, ending the isolation with a digestion with DNaseI. For each sample, 500 ng of total RNA were converted into cDNA using oligo(dT) and M-MLV reverse transcriptase (Promega, Madison, WI, USA) according to the manufacturer's recommendation.

The transcript expression of *Bv*PIP2;1, *Bv*PIP2;2, *Bv*PIP1;1, *Bv*UBIep and *Bv*GAPDH genes was studied by real-time polymerase chain reaction (RT-PCR). The primers were designed based on published sequences of the aquaporins found in *B. vulgaris* **[see Supporting Information—Table S2]**. The selection of *Bv*UBlep and *Bv*GAPDH as the housekeeping genes was based on genes reported in *B. vulgaris*

and information available in the literature (Reid *et al.* 2006; Wan *et al.* 2010). The mRNA abundance of *Bv*GAPDH and *Bv*UBIep was not significantly different between the treatments (data not shown).

Quantitative PCR (qPCR) was performed with a MyiQ cycler (Bio-Rad) in a reaction volume of 25 μL containing 12.5 μL of IQ Sybr Green Super Mix (Bio-Rad), 320 nM primers and 5 μL of a 1/500 dilution of cDNA. The RT qPCR conditions comprised 1 cycle at 95 °C for 5 min and 34 cycles at 95 °C for 45 s, 60 °C for 30 s and 72 °C for 1 min. Amplification data were collected during the extension step (72 °C). The efficiency of the primer binding was determined by linear regression by plotting the cycle threshold value versus the log of the cDNA dilution (Soto *et al.* 2010). The absolute RNA amount for each gene was determined in every qPCR experiment. The relative gene expression was calculated as the ratio of the initial gene quantity to the initial mean quantity of the housekeeping genes (Soto *et al.* 2011). Quantitative PCR experiments were independently performed three times with comparable results. The three PCR reactions were carried out in duplicate. The transcript levels of the three studied aquaporins under salt treatments were compared with an osmotic treatment imposed by a non-charge and non-permeable solute [polyethylene glycol (PEG) 6000] at a concentration of 23 % (*p/v*), which induces a Ψ_{medium} of −0.90 MPa. The purpose was to contrast aquaporin transcripts between ion signals (NaCl and KCl) versus non-charged non-permeable osmolyte (data not shown).

Restoring salt-treated plants to control medium: L_{pr} and g_s recovery profiles

To measure the L_{pr} and g_s recovery profiles, the plants were first submitted to a salt treatment (200 mM NaCl or KCl) for 4 or 24 h and then transferred to a control solution (considered now $t = 0$ h). Root hydraulic conductivity and g_s were then measured at different time intervals (0, 1 and 24 h) to characterize the plant's capacity to restore L_{pr} and g_s when the salt treatment was halted. As a control, we first determined the L_{pr} values immediately after changing the detopped roots to a control medium. This protocol was crucial to discard the flows that could be artefacts due to injury exacerbated with the salinity treatment. Root hydraulic conductivity values in control medium were not significantly different from those measured in the saline treatment **[see Supporting Information—Graph S2]**. All values shown are the average of three independent experiments. In each experiment, g_s was measured in one leaf per plant in three different plants and two or three roots were detopped for measuring L_{pr} under each condition.

Statistical analysis

Statistical analysis was performed using software GraphPad Prism 5.00 for Windows, GraphPad Software, San Diego, CA, USA, www.graphpad.com. Differences were accepted as significant with at least $P < 0.05$ employing analysis of variance (ANOVA) and Bonferroni tests as indicated in the figure legends.

Results

Characterization of a new state for *B. vulgaris* under salt stress

Salt stress was achieved by the addition of 200 mM NaCl ($\Psi_{medium} = -0.90$ MPa). Under this condition, plants were able to rapidly show a clear change in their phenotype (loss of turgor) followed by a gain in turgor in <24 h (Fig. 1). The phenotype observed in plants exposed to 200 mM KCl was indistinguishable from the NaCl treatment (Fig. 1A), and no chlorosis symptoms were observed in the leaf. As expected, the tolerant phenotype shows a reduction in transpiration rate and in the leaf RGR in both salt treatments, although growth was not arrested **[see Supporting Information—Graph S3]**. Moreover, during the whole experiment, the shoot–root ratio was not significantly modified, so the growth rate changes in the leaf were also translated to the root growth rate (Fig. 1B).

The water status of the hydroponically grown *B. vulgaris* plants was characterized. The RWC was reduced according to the phenotype observed (Fig. 1C). The Ψ'_{leaf} was analysed at different time intervals (0, 4, 8, 24 and 48 h) for the control and treated plants. The mean Ψ'_{leaf} in the control plants was -0.17 ± 0.02 MPa and remained constant during the whole experiment (Fig. 1D). When Ψ'_{leaf} was measured after 4 h of the onset of the stress treatment, its mean value was significantly reduced in the NaCl condition (-0.20 ± 0.03 to -0.74 ± 0.01 MPa) and in the KCl condition (-0.19 ± 0.02 to -0.79 ± 0.01 MPa). The initial drop in Ψ'_{leaf} is well correlated with plant turgor loss in both salt treatments (Fig. 1A). The Ψ'_{leaf} remained at these low values up to 48 h although the turgid phenotype changed (Fig. 1). The leaf Ψ_{osm} remained constant in the control plants and showed a reduction in the plants submitted to stress after 24 h **[see Supporting Information—Table S1]**. The patterns of Ψ_p versus time were well correlated with the observed phenotype of loss and gain in turgor (Fig. 1A and E).

All of these parameters allowed us to define two distinguishable time intervals in terms of water adjustment during salt stress response, 4 h, where there is loss of turgor and 24 h, where there is gain of turgor. Our next step was to analyse these two conditions in terms of overall hydraulic adjustments.

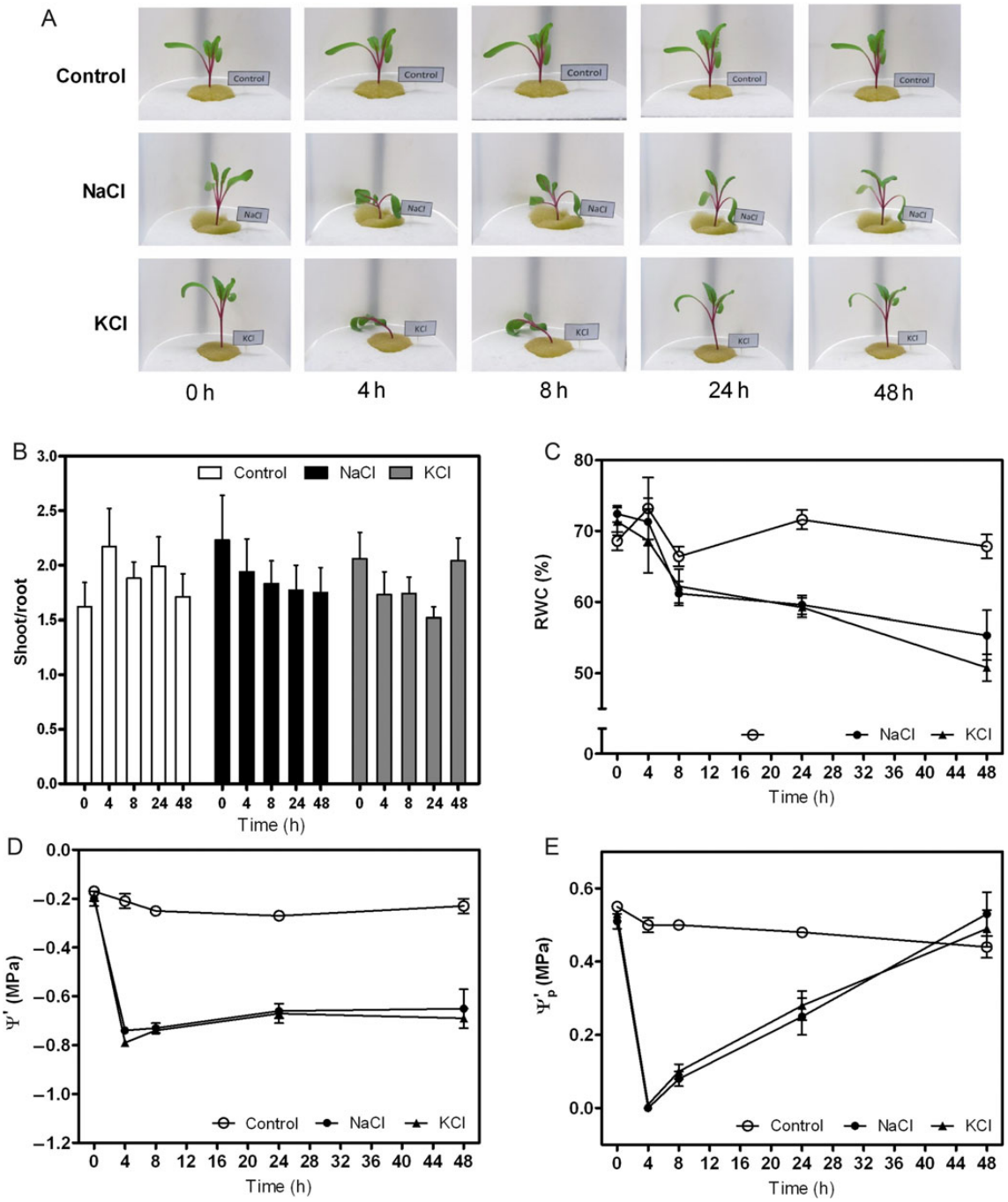

Figure 1. Effect of salinity treatments on *B. vulgaris* plants: control ($\Psi_{medium} = -0.04$ MPa); 200 mM NaCl ($\Psi_{medium} = -0.90$ MPa) or 200 mM KCl ($\Psi_{medium} = -0.90$ MPa). (A) Images of the same hydroponically grown plant taken in each condition at the indicated times after the onset of the treatment. (B) Shoot–root ratio values are given as bars representing mean ± SE of three independent experiments ($n = 3$). The biological replicates were five to six plants per treatment in each experiment. No differences were observed between treatments ($F_{(2,68)} = 0.16$, $P = 0.8513$). (C) Relative water content values are expressed as mean ± SE of three independent experiments ($n = 3$). The biological replicates were three plants per treatment in each experiment, and two leaves per plant were analysed as a duplicate. (D) The Ψ'_{leaf} values (in MPa) measured at each indicated time are expressed as mean ± SE of three independent experiments. (E) The calculated apparent leaf pressure potential (Ψ'_p in MPa) is expressed as mean values ± SE.

Linking root hydraulic response to the overall SPAC

As expected, the salt added to the medium triggered a rapid decrease in g_s, which remained low even up to 24 h (Fig. 2A). In the control conditions, the plants showed mean L_{pr} values of 72.3 ± 21.1 mL g^{-1} h^{-1} MPa^{-1} (Fig. 2B). Both salt treatments induced a rapid and indistinguishable decrease

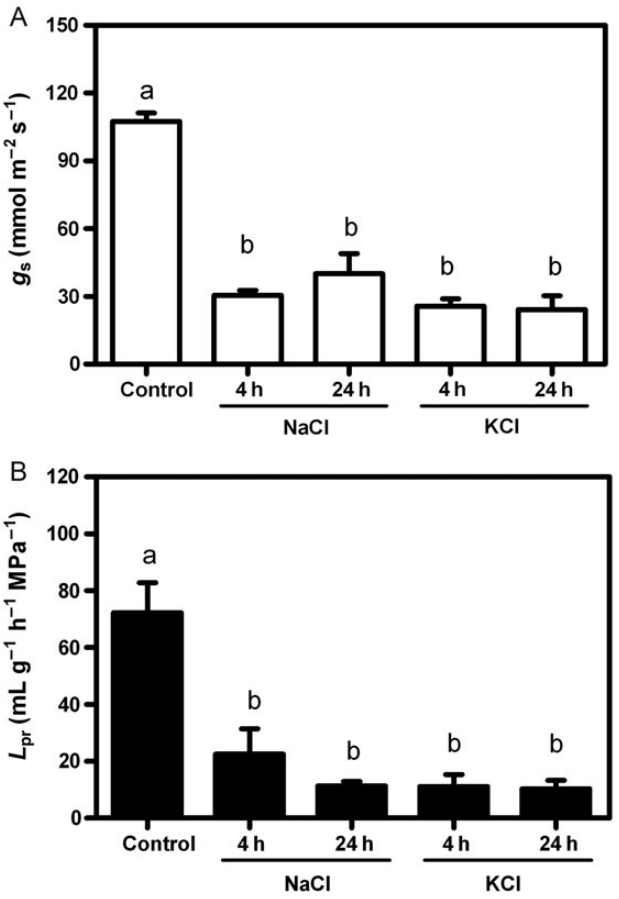

Figure 2. Integrating SPAC key points: g_s and L_{pr}. (A) Stomatal conductance values (g_s, in mmol m^{-2} s^{-1}) are given as bars representing mean ± SE of three independent experiments (at least three plants per treatment). Different letters indicate statistical differences between treatments ($P < 0.001$; Bonferroni test). (B) Hydraulic conductivity values (L_{pr}; in mL mg^{-1} h^{-1} MPa^{-1}) are given as bars representing mean ± SE of three independent experiments (in each one, two to three individual root systems were measured). Different letters indicate statistical differences between treatments ($P < 0.001$; Bonferroni test).

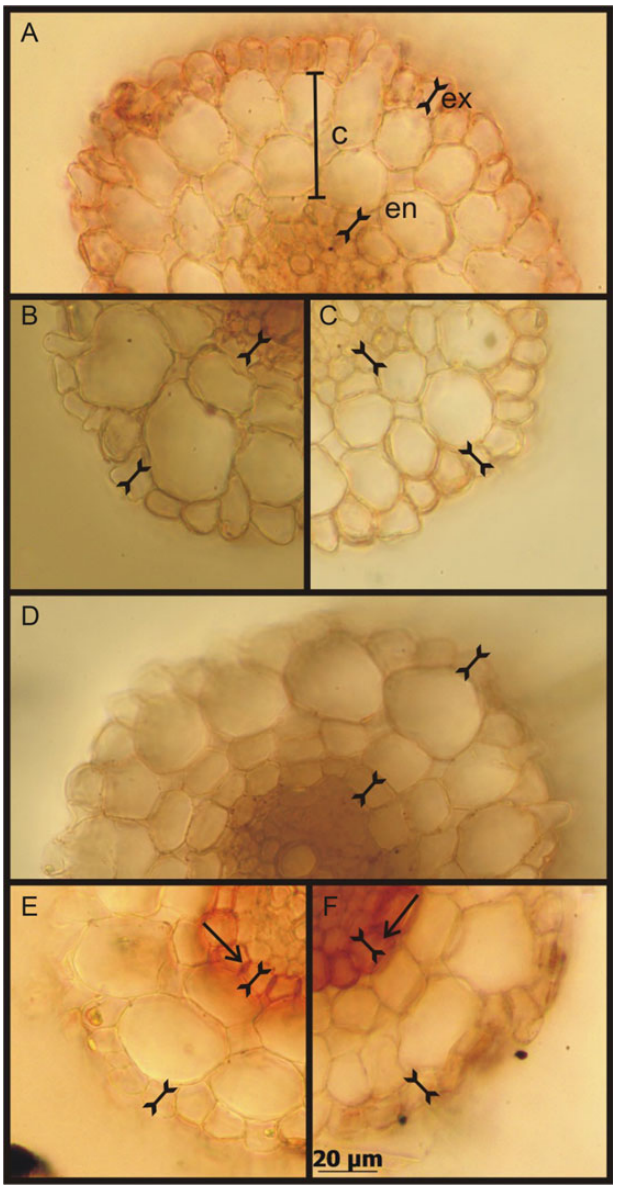

Figure 3. Photographs of *B. vulgaris* fresh root cross-sections stained with Sudan IV, the bar represents 20 µm. (A and D) Control root cuts indicating cortex (C), endodermis (en) and exodermis (ex). (B and C) Representative cuts of roots from plants treated for 4 h with 200 mM NaCl and 200 mM KCl, respectively. (E and F) Representative cuts of roots from plants treated for 24 h with 200 mM NaCl and 200 mM KCl, respectively. The arrows show suberization of endodermis. The images are one sample per condition of 10 independent experiments ($n = 10$).

in L_{pr}. The L_{pr} inhibition was 80 % compared with the control condition after 4 h of treatment, and this low L_{pr} value was maintained up to 24 h of treatment. The g_s modifications are similar to the profile shown by L_{pr}, suggesting that the change in the root water flow is coupled to g_s.

Exploring root adjustments in terms of water pathways

The anatomical changes and the presence of aquaporins provide some insight into the putative involvement of the different water pathways at the root level for the two selected time intervals (4 and 24 h of treatment in 200 mM NaCl or 200 mM KCl). We, therefore, incubated root sections in the presence of Sudan IV in order to check suberization (Fig. 3). The plant roots challenged by either NaCl or KCl for a period of 4 h showed undetectable suberization changes of the endodermis and/or exodermis, as in the control plants. For longer exposures (24 h), the suberization of the endodermis increased independently of the ion treatment (Fig. 3E and F), whereas the control roots do not present enhanced intensity for Sudan IV. Similar results were observed when the

autofluorescence of the cell wall was analysed (data not shown). These clear changes observed in the endodermis suberization were not observed in the exodermis. The exodermis suberization was very low and random, mostly attributable to higher thickness in the fresh cuts (Fig. 3A).

Quantitative RT-PCR analysis was performed to accurately determine the transcript levels of the PIP genes *Bv*PIP2;1, *Bv*PIP2;2 and *Bv*PIP1;1 in whole roots under salt stress (NaCl or KCl, Fig. 4) at different time intervals. *Bv*PIP2;1 might have a circadian behaviour as described in other PIPs (Takase *et al.* 2011; Caldeira *et al.* 2014).

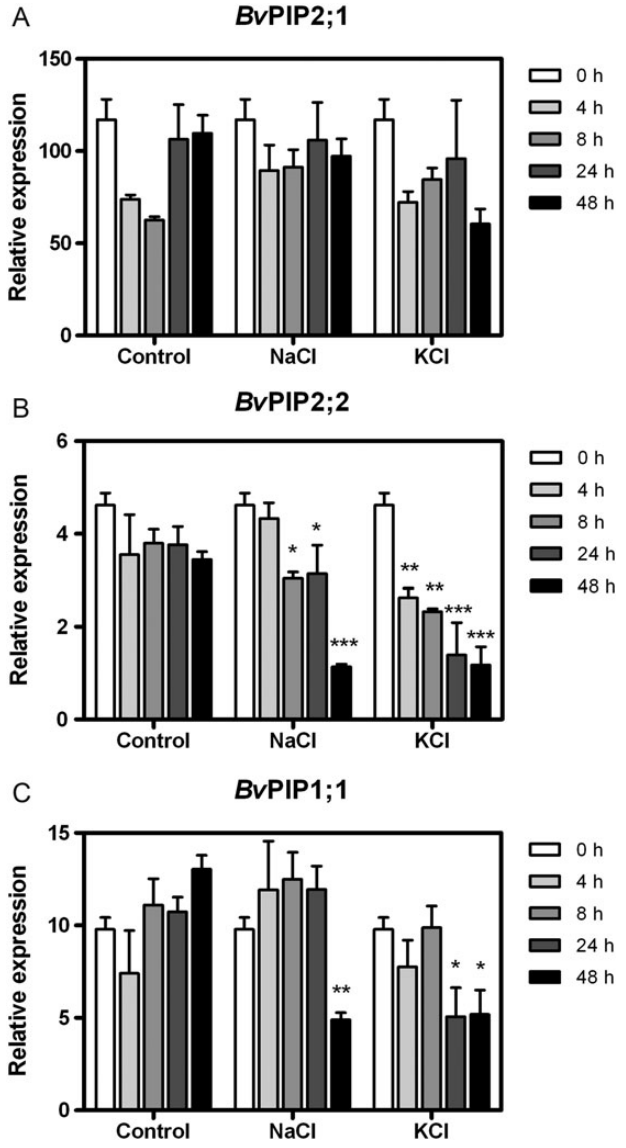

Figure 4. Relative gene expression of *Bv*PIP2;1 (A), *Bv*PIP2;2 (B) and *Bv*PIP1;1 (C) in roots from control, 200 mM NaCl or 200 mM KCl treatments. Data are given as bars representing mean values ± SE of three independent experiments ($n = 3$), and asterisks indicate statistical differences from initial condition ($t = 0$ h) for each treatment (*$P < 0.05$; **$P < 0.01$; ***$P < 0.001$; Bonferroni test) **[see Supporting Information—Tables S3–S5** for statistical analysis].

The studied aquaporins showed a subtle down-regulation profile, except the relative expression level of *Bv*PIP2;1, which did not decrease at all, independently of the treatment (Fig. 4A, **see Supporting Information—Tables S3–S5** for the statistical analyses). Interestingly, the profile of the *Bv*PIP2;2 and *Bv*PIP1;1 expressions for the NaCl stress condition did not show down-regulation at the same pace as observed in the KCl stress (Fig. 4B and C). The differences of the ion treatments became more evident for *Bv*PIP1;1, which showed down-regulation at 24 h when the plants were exposed to KCl, while the decrease became significant at 48 h under NaCl stress (Fig. 4C and **see Supporting Information—Tables S3–S5** for the statistical analyses).

To determine whether the lack of a strong down-regulation of these three aquaporins is only observed under salt treatment, the salt was replaced by a non-permeable and non-charged molecule as PEG. The plants submitted to $\Psi_{medium} = -0.90$ MPa generated with PEG triggered an expression decrease of 56–67 % in these aquaporins after 4 h of treatment, a strong transcript down-regulation compared with both salt treatment (NaCl versus PEG: $P < 0.001$, KCl versus PEG: $P < 0.05$, Bonferroni post-test).

Restoring salt-treated plants to control medium: L_{pr} and g_s recovery

Our results confirm that the root water pathways are different in the two selected intervals (4 and 24 h) and that the three studied aquaporins are relatively stable upon salt treatments and only strongly down-regulated when a non-charge solute is imposed. However, the results do not allow us to completely dissociate the water pathways and ion redistribution (NaCl versus KCl). We decided to explore whether halting the salt treatment allows us to describe the shoot–root water dynamics through the analysis of g_s and L_{pr} recovery.

As shown in Fig. 5, the g_s recovery profile of the plants returned to the control medium reflected dependence of the time of the preceding salt treatment and dependence of the ion involved in the salt treatment. Thus, g_s recovered faster in the 4-h salt-treated plants than in the 24-h salt-treated plants (Fig. 5A and B). The 4-h salt-treated plants restored to the control solution for 1 h were able to increase $g_s \cong 50$ % with respect to the g_s values before halting the treatment (Fig. 5A). In this analysed point (4 h of salt treatment before the halting), the recovery trend is independent of the involved cation (NaCl versus KCl; $F_{(1,22)} = 3.06$, $P = 0.0940$, two-way ANOVA). The plants subjected to NaCl or KCl for 24 h differed in their kinetic to increase g_s when they were restored to the control medium. In this condition (24 h of salt treatment), the ion involved in the salt stress significantly affects the recovery profile of g_s (ion accounts for

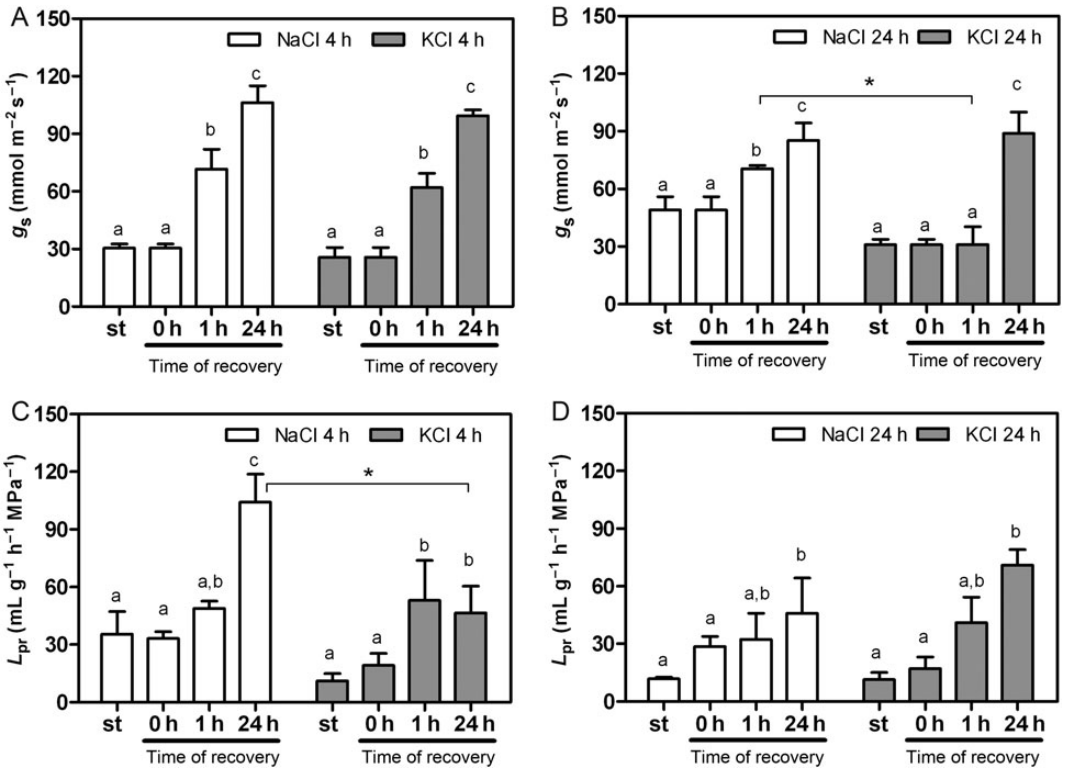

Figure 5. Recovery profile of g_s (A and B) and L_{pr} (C and D) after halting the salt treatment (st). The recovery profiles are separated for plants initially submitted to short salt treatments ($t = 4$ h, A and C) versus a longer interval period ($t = 24$ h, B and D). Data are expressed as mean values $\pm$ SE of three to four independent experiments (in each one, three to four plants were measured). Different letters indicate statistical differences between bars ($P < 0.05$; Bonferroni test), and an asterisk indicates differences between bars from different salt treatments ($P < 0.001$, Bonferroni test).

13.25 % of total variance, $F_{(1,16)} = 12.99$, $P = 0.0024$, two-way ANOVA). Even though g_s reached the same final value after 24 h of recovery in control solution, the recovery trend of g_s is much faster in NaCl-treated plants than in KCl-treated plants (Fig. 5B).

Conversely, the L_{pr} recovery profile of the plants restored to the control medium reflected a completely different strategy in terms of time dependence and ion dependence with respect to g_s. Moreover, the recovery patterns of both hydraulic parameters (g_s and L_{pr}) seem to be uncoupled although both presented a coupled reduction in salt treatment (Figs 5 and 6). In the first analysed condition (4 h of salt treatment), the recovery trend of L_{pr} is significantly affected by the ion involved before halting stress (Fig. 5C, $F_{(1,17)} = 8.62$, $P = 0.0092$). The 4-h KCl-treated plants turned into control solution showed a quick L_{pr} increment that remained unchanged for 24 h. In 4-h NaCl-treated plants, L_{pr} gradually rose to higher values (*$P < 0.001$; Bonferroni test). For the 24-h-treated plants, the trend of L_{pr} increment was independent of the salt treatment ($F_{(1,16)} = 0.58$, $P = 0.4588$, Fig. 5D). In the case of the NaCl-treated plants, L_{pr} recovery was affected by the extension of treatment (4 versus 24 h; Fig. 5C and D). The 4-h salt-treated plants presented a significantly higher L_{pr} value ($P < 0.05$; Bonferroni test) after 24 h of restoring the plants to the control solution. On the contrary, in the case of the KCl-treated plants, the L_{pr} recovery profile is independent of the extension of the treatment, i.e. 4 or 24 h (Fig. 5C and D). The 4-h-treated and 24-h-treated plants presented a similar L_{pr} value after 1 h of restoring the plants to the control solution, which was significantly different from the L_{pr} value observed under salt stress. Figure 6 illustrates g_s and L_{pr} recovery profile observed for the four conditions (NaCl or KCl; and/or the selected time points, 4 and 24 h).

Discussion

Water homeostasis is linked to ion redistribution in plants as an important defence strategy against salt stress (Tester and Davenport 2003; Shabala and Cuin 2008; Shabala 2013; Flowers and Colmer 2015). *Beta vulgaris* showed great plasticity reflecting its ability to rapidly gain turgor due to osmotic adjustment, consistent with the maintenance of a low Ψ'_{leaf} during the entire treatment (Fig. 1). Under our experimental conditions, low

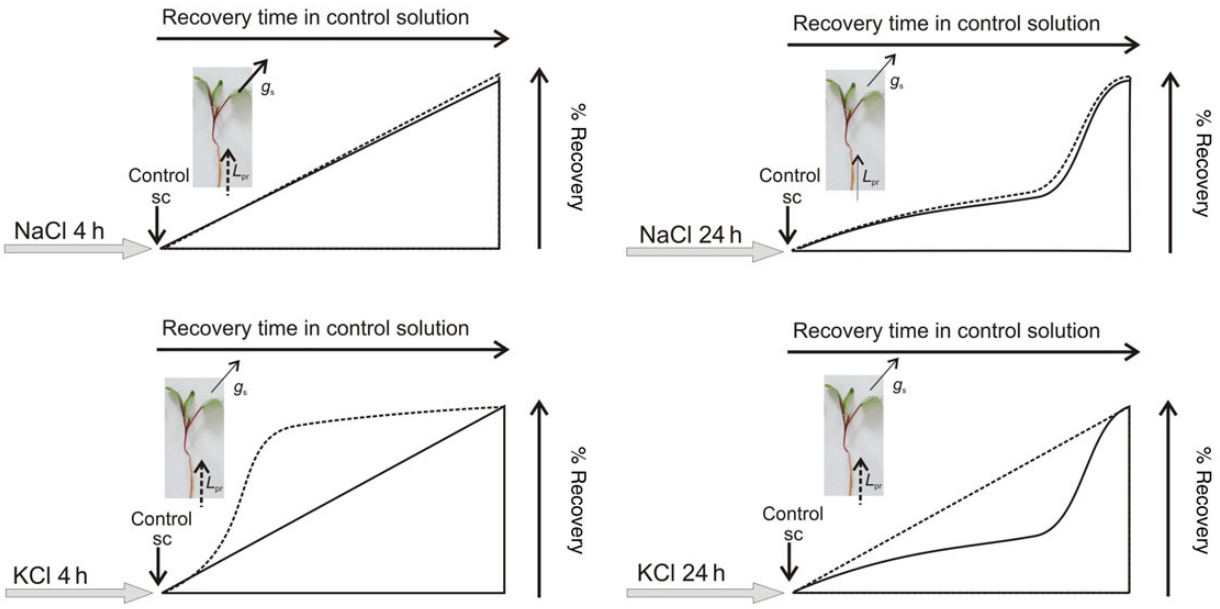

Figure 6. Schematic representation of recovery profiles of L_{pr} (dotted line) and g_s (continuous line) after stress treatments.

RWC values—even for plants gaining turgor after 24 h of salt treatment—might be associated with an underestimation of the RWC as a result of an osmotic adjustment **[see Supporting Information—Table S1]**. The gain of turgor under salt treatment requires solute synthesis and/or recirculation of cations, and this should also be reflected in the obtained RWC values (Weatherley 1950; Boyer *et al.* 2008). The aerial parts only modified 1 % of the water content (data not shown), even in the phenotype that lost turgor (4 h of salt treatment; Fig. 1), a trait consistent with an isohydric-like behaviour (Sade and Moshelion 2014). Thus, the overall strategy is successful for the adjustment of the water content. These data are supported by other studies performed using members of the Chenopodiaceae family under salt stress (Lindhauer *et al.* 1990; Ghoulam *et al.* 2002; Pakniyat and Armion 2007; Abbas *et al.* 2012), where Ψ_{osm} is the key element in turgor recovery. In our experimental design, the analyses were performed at 4 h (loss of turgor) and 24 h (gain of turgor) of salt treatment because these are two distinguishable transition states before a new water plant status is achieved.

The transpiration rate and L_{pr} have not always been reported as a coupled process. For instance, changes in shoot transpiration are not reflected by changes in L_{pr} in *Lotus japonicus* (Henzler *et al.* 1999), while in wheat, it was reported an important correlation between increasing L_{pr}, the cortex cell hydraulic conductivity, transpiration and the root expression of aquaporins—*Ta*PIP1;2 and *Ta*PIP2;5 (Wang *et al.* 2013). Our results clearly showed that under salt treatment, there is a correlated decrease in g_s and root hydraulic properties (L_{pr}) (Fig. 2), as both parameters presented an 80 % reduction compared with the control condition. The decrease in g_s (Fig. 2A) remained low even up to 24 h, which is consistent with the decrease in the leaf water potential values (Fig. 1D). This occurs for both NaCl and KCl treatments and is in agreement with observations performed in other species, such as wheat, that similarly decreased their g_s when exposed to either NaCl or KCl (Rahnama *et al.* 2010). The transition of the phenotypes—loss (4 h) and gain (24 h) of turgor—is not reflected in the two key water balance modulators (L_{pr} and g_s) that remained coupled and similarly low. The hydraulic parameters only reflect a centred strategy of water loss avoidance.

Thus, it is necessary to explore how the root copes with water loss not only in terms of hydraulic properties but also in the analysis of the water pathways. The L_{pr} decrease (Fig. 2B) in our experimental set-up was consistent with other observations for different species (Martínez-Ballesta *et al.* 2003; Boursiac *et al.* 2005; Postaire *et al.* 2010; Muries *et al.* 2011). The roots showed a marked ability to adjust their L_{pr} during the first 4 h of treatment (our first hydraulic transition point) even before plants display any anatomical or morphological change (Fig. 3). It is consistent with faster responses that are usually present in the initial time lapse response to tolerance (Horie *et al.* 2012). In both 4 h salt treatments (NaCl and KCl), the suberization is indistinguishable from the control plants. The root apoplastic pathways were not modified, so the cell-to-cell pathway could be limiting (or maximizing) root resistance to the water flows both in favour of (or restricting) water entry and/or exit. Thus, membrane permeability not only to ions but also to water can contribute to plasticity together with the change

in xylem tension as a consequence of the decrease in leaf water potential.

In our second hydraulic transition point (24 h treatment), the low L_{pr} values involved also an anatomical restriction enhancing the hydraulic resistance to water flows along the roots, suggesting an increment in the water flows through the cell-to-cell pathways (a more resistive pathway). The increase in suberization observed after 24-h treatment can be attributed to a completely different strategy. This is consistent with recent reports demonstrating that the cell-to-cell pathway might contribute significantly to the radial water uptake particularly during development (Knipfer and Fricke 2010; Knipfer *et al.* 2011; Gambetta *et al.* 2012, 2013; Caldeira *et al.* 2014; Suku *et al.* 2014). In wheat plants, a non-membranous pathway (apoplast) contributes to increase radial water uptake in the control but not in the NaCl-stressed plants (Fricke *et al.* 2013).

It is possible that the effectiveness of *B. vulgaris* to tolerate the saline stress could be associated with its capacity to maintain the expression level of the AQPs in the salt treatments (Fig. 4), as reported for other specific proteins strictly involved in salt tolerance (Chinnusamy *et al.* 2004, 2006). This statement cannot be made with certainty because aquaporin activity and protein expression were not tested here. The root strategy to maintain water flow is based on water and ion redistribution and adjusting the cell-to-cell pathway by means of its selected membrane permeability (Steudle 2000). A solely osmotic stress (PEG solute) shuts down the transcripts of the *Bv*PIP characterized in <4 h of treatment, which might contribute by increasing the root cell resistance to the water pathway. On the contrary, the cell-to-cell pathway in salt-treated *B. vulgaris* plants might contribute by increasing the capability to regulate water transfers because water permeability can be tuned to limiting (or maximizing) the resistance in concert with ion redistribution.

We could experimentally dissociate L_{pr} from g_s employing two strategies: (i) different cations—Na^+ versus K^+—to promote the stress and (ii) analysing L_{pr} enhancement when the salt treatment is interrupted (Fig. 5). Most of the studies in the literature are based on the analysis of L_{pr} decrease by means of an imposed stress condition or the presence of aquaporin inhibitors (e.g. Ehlert *et al.* 2009; Vandeleur *et al.* 2009). To our knowledge, this is the first work that explored altogether L_{pr} decrease and enhancement, as most of the works show L_{pr} inhibition and not its recovery. Whereas K^+ and Na^+ have distinct redistribution profiles, different L_{pr} recovery pathways for water are expected to be involved even in the presence of an equivalent change in the driving force along the SPAC for both situations. After stress treatments, the recovery of both hydraulic parameters (L_{pr} and g_s) denoted two different strategies (Fig. 6). The enhancement in L_{pr} shows a profile (Figs 5C and 6) that is linked to ion redistribution (Na^+ versus K^+) and this is part of the root plasticity to prevent water loss. In the first transition point (4 h of salt treatment), the cation dependence of the L_{pr} profile highlights the participation of membrane permeability in root plasticity together with the change in xylem tension. On the other hand, L_{pr} recovery profiles observed after 24 h of salt treatment suggest that under our experimental conditions, root resistance to water flow does not differ between the ion source of the stress (Na^+ or K^+). This is consistent with an increase in the total root resistance and the observed strong endodermis suberization in both salt treatments (Fig. 3E and F). The recovery profile of NaCl treatments shows a coupled temporal dependence strategy where g_s and L_{pr} increase at the same rate. Both parameters increase at a slower pace when the plants were treated for 24 h compared with 4 h. Conversely, g_s and L_{pr} enhancement are clearly uncoupled in the KCl treatments (Fig. 6). The root shows the capacity to restore the water transport capacity before the water is transpired through stomata. It is well described in the literature that under salt stress, Na^+ is redistributed to avoid toxicity, while K^+ functions as an interchangeable ion all along the vasculature (particularly phloem) (Peng *et al.* 2004; Munns and Tester 2008; Karley and White 2009; Shabala *et al.* 2010; Flowers and Colmer 2015). In this context, the potassium gradient might be crucial in the root–shoot hydraulic signalling (Gajdanowicz *et al.* 2011). The profiles observed in Fig. 6 are consistent with sustaining a 'hydraulic' adjustment in the presence of NaCl compared with a 'tuned' adjustment caused by the redistribution in the case of KCl, which is clearly reflected in g_s and L_{pr} changes.

The proposed initial two set points—4 and 24 h extension in the imposed salt treatment—were selected because of the triggered distinguishable phenotypes in *B. vulgaris*. At 4 h of an imposed 200 mM salt stress, plants have lost turgor and osmotic adjustment has not been completed. In this situation, the L_{pr} recovery profile suggests a much higher root tuning capacity to modulate the water dynamics that affects the whole-plant water loss avoidance strategy. At 24 h of 200 mM salt stress, plants are gaining turgor, and the L_{pr} recovery profile suggests that the root versatility is more restricted as tolerance has already been triggered.

Conclusions

Tolerance involves limiting water movement by increasing the total plant hydraulic resistance. *Beta vulgaris* osmotic adjustment is sustained by tuning L_{pr} and g_s.

Our work presents a quantitative analysis of the coordinated link between L_{pr} and g_s when the ion and water redistribution strategy takes place. Even when the xylem tension and apoplast pathway mediate plant water flows, the cell-to-cell pathway contributes as a key component to the capacity to transport water per unit surface and driving force in the SPAC (nicely demonstrated in the enhancement of L_{pr} after halting KCl treatment). Future research should explore the molecular basis for the different strategies that plants use to regulate their water balance and identify the imposed threshold of the cell-to-cell pathways in terms of hydraulic resistance.

Sources of Funding

This work was supported by the Agencia Nacional para la Promoción Científica y Técnica [Préstamo BID PICT11-2239 and PICT14-0744], Consejo de Investigaciones Científicas y Técnicas (CONICET) Proyecto de Investigación Plurianual (PIP12-14) and Universidad de Buenos Aires UBACyT14-17, all grants to G.A.

Contributions by the Authors

V.V., J.B. and G.A. were involved in the study conception and design. V.V. and J.B. planned and performed experiments and analysed data. J.B., G.S. and N.D.A. additionally participated in the design and data acquisition of the qRT-PCR experiments. V.V. and G.A. were involved in the analysis and interpretation of the data, discussion and writing the manuscript. All authors had intellectual input into the project.

Conflict of Interest Statement

None declared.

Acknowledgements

We thank Milena Manzur, Moira Sutka, Agustín Yaneff, Esteban Tubert, Karina Alleva and Cintia Jozefkowicz for critical comments in the manuscript. We also thank the anonymous reviewers and all the editors for their helpful comments and suggestions on this paper.

Supporting Information

The following additional information is available in the online version of this article –

Figure S1. Different concentrations of salt treatments.

Table S1. Osmotic potential measured for the leaf sap.

Graph S1. Root hydraulic conductivity determination.

Table S2. Accession number of genes and sequences of primer pairs used for qRT-PCR.

Graph S2. Root hydraulic conductivity determination after halting salt treatment.

Graph S3. Plant transpiration rate and RGR of leaf area.

Tables S3–S5. Quantitative real-time polymerase chain reaction statistical analysis.

Literature Cited

Abbas F, Mohanna A, Al-Lahham Gh, Al-Jbawi E. 2012. Osmotic adjustment in sugar beet plant under salinity stress. *Journal of Sugar Beet* **28**:37–43.

Alleva K, Niemietz CM, Sutka M, Maurel C, Parisi M, Tyerman SD, Amodeo G. 2006. Plasma membrane of *Beta vulgaris* storage root shows high water channel activity regulated by cytoplasmic pH and a dual range of calcium concentrations. *Journal of Experimental Botany* **57**:609–621.

Alleva K, Chara O, Amodeo G. 2012. Aquaporins: another piece in the osmotic puzzle. *FEBS Letters* **586**:2991–2999.

Barone LM, Shih C, Wasserman BP. 1997. Mercury-induced conformational changes and identification of conserved surface loops in plasma membrane aquaporins from higher plants. Topology of PMIP31 from *Beta vulgaris* L. *Journal of Biological Chemistry* **272**:30672–30677.

Barone LM, Mu HH, Shih CJ, Kashlan KB, Wasserman BP. 1998. Distinct biochemical and topological properties of the 31- and 27-kilodalton plasma membrane intrinsic protein subgroups from red beet. *Plant Physiology* **118**:315–322.

Bartels D, Dinakar C. 2013. Balancing salinity stress responses in halophytes and non-halophytes: a comparison between *Thellungiella* and *Arabidopsis thaliana*. *Functional Plant Biology* **40**:819–831.

Bartels D, Sunkar R. 2005. Drought and salt tolerance in plants. *Critical Reviews in Plant Science* **24**:23–58.

Bellati J, Alleva K, Soto G, Vitali V, Jozefkowicz C, Amodeo G. 2010. Intracellular pH sensing is altered by plasma membrane PIP aquaporin co-expression. *Plant Molecular Biology* **74**:105–118.

Boursiac Y, Chen S, Luu DT, Sorieul M, Van den Dries N, Maurel C. 2005. Early effects of salinity on water transport in *Arabidopsis* roots. Molecular and cellular features of aquaporin expression. *Plant Physiology* **139**:790–805.

Boursiac Y, Boudet J, Postaire O, Luu DT, Tournaire-Roux C, Maurel C. 2008. Stimulus-induced downregulation of root water transport involves reactive oxygen species-activated cell signalling and plasma membrane intrinsic protein internalization. *The Plant Journal* **56**:207–218.

Boyer JS. 1969. Free-energy transfer in plants. *Science* **163**:1219–1220.

Boyer JS, James RA, Munns R, Condon AG, Passioura JB. 2008. Osmotic adjustment leads to anomalously low estimates of relative water content in wheat and barley. *Functional Plant Biology* **35**:1172–1182.

Bramley H, Turner NC, Turner DW, Tyerman SD. 2009. Roles of morphology, anatomy, and aquaporins in determining contrasting hydraulic behavior of roots. *Plant Physiology* **150**:348–364.

Caldeira CF, Bosio M, Parent B, Jeanguenin L, Chaumont F, Tardieu F. 2014. A hydraulic model is compatible with rapid changes in leaf elongation under fluctuating evaporative demand and soil water status. *Plant Physiology* **164**:1718–1730.

Chaumont F, Tyerman SD. 2014. Aquaporins: highly regulated channels controlling plant water relations. *Plant Physiology* **164**:1600–1618.

Chinnusamy V, Schumaker K, Zhu JK. 2004. Molecular genetic perspectives on cross-talk and specificity in abiotic stress signalling in plants. *Journal of Experimental Botany* **55**:225–236.

Chinnusamy V, Zhu J, Zhu JK. 2006. Salt stress signaling and mechanisms of plant salt tolerance. *Genetic Engineering: Principles and Methods* **27**:141–177.

Clarke NA, Hetschkun H, Jones C, Boswell E, Marfaing H. 1993. Identification of stress tolerance traits in sugar beet. In: Jackson MB, Black CR, eds. *Interaction stresses on plants in a changing climate*. Berlin: Springer, 511–529.

Daoud S, Harrouni C, Huchzermeyer B, Koyro HW. 2008. Comparison of salinity tolerance of two related subspecies of *Beta vulgaris*: the sea beet (*Beta vulgaris* ssp. *maritima*) and the sugar beet (*Beta vulgaris* ssp. vulgaris). In: Abdelly C, Öztürk M, Ashraf M, Grignon C, eds. *Biosaline agriculture and high salinity tolerance*, Part Section I. Basel: Birkhäuser Publisher, 115–129.

Dohm JC, Minoche AE, Holtgräwe D, Capella-Gutiérrez S, Zakrzewski F, Tafer H, Rupp O, Sörensen TR, Stracke R, Reinhardt R, Goesmann A, Kraft T, Schulz B, Stadler PF, Schmidt T, Gabaldón T, Lehrach H, Weisshaar B, Himmelbauer H. 2014. The genome of the recently domesticated crop plant sugar beet (*Beta vulgaris*). *Nature* **505**: 546–549.

Ehlert C, Maurel C, Tardieu F, Simonneau T. 2009. Aquaporin-mediated reduction in maize root hydraulic conductivity impacts cell turgor and leaf elongation even without changing transpiration. *Plant Physiology* **150**:1093–1104.

Finkelstein R. 2013. Abscisic acid synthesis and response. *The Arabidopsis Book* **11**:e0166.

Flowers TJ, Colmer TD. 2015. Plant salt tolerance: adaptations in halophytes. *Annals of Botany* **115**:327–331.

Fricke W, Bijanzadeh E, Emam Y, Knipfer T. 2013. Root hydraulics in salt-stressed wheat. *Functional Plant Biology* **41**:366–378.

Fritz M, Lorenzen S, Popova M, Ehwald R. 2010. Transient and permanent changes of xylem sap exudation by root systems of *Zea mays* after application of hydrostatic and osmotic forces. *Functional Plant Biology* **37**:813–827.

Gajdanowicz P, Michard E, Sandmann M, Rocha M, Corrêa LG, Ramírez-Aguilar SJ, Gomez-Porras JL, González W, Thibaud JB, Van Dongen JT, Dreyer I. 2011. Potassium (K^+) gradients serve as a mobile energy source in plant vascular tissues. *Proceedings of the National Academy of Sciences of the USA* **108**:864–869.

Galvan-Ampudia CS, Testerink C. 2011. Salt stress signals shape the plant root. *Current Opinion in Plant Biology* **14**:296–302.

Gambetta GA, Manuck CM, Drucker ST, Shaghasi T, Fort K, Matthews MA, Walker MA, Mcelrone AJ. 2012. The relationship between root hydraulics and scion vigour across Vitis rootstocks: what role do root aquaporins play? *Journal of Experimental Botany* **63**:6445–6455.

Gambetta GA, Fei J, Rost TL, Knipfer T, Matthews MA, Shackel KA, Walker MA, Mcelrone AJ. 2013. Water uptake along the length of grapevine fine roots: developmental anatomy, tissue-specific aquaporin expression, and pathways of water transport. *Plant Physiology* **163**:1254–1265.

Geng Y, Wu R, Wee CW, Xie F, Wei X, Chan PMY, Tham C, Duan L, Dinneny JR. 2013. A spatio-temporal understanding of growth regulation during the salt stress response in *Arabidopsis*. *The Plant Cell* **25**:2132–2154.

Ghoulam C, Foursy A, Fares K. 2002. Effects of salt stress on growth, inorganic ions and proline accumulation in relation to osmotic adjustment in five sugar beet cultivars. *Environmental and Experimental Botany* **47**:39–50.

Hachez C, Chaumont F. 2010. Aquaporins: a family of highly regulated multifunctional channels. *Advances in Experimental Medicine and Biology* **679**:1–17.

Hachez C, Zelazny E, Chaumont F. 2006. Modulating the expression of aquaporin genes in planta: a key to understand their physiological functions*? Biochimica et Biophysica Acta (BBA) - Biomembranes* **1758**:1142–1156.

Hachez C, Veselov D, Ye Q, Reinhardt H, Knipfer T, Fricke W, Chaumont F. 2012. Short-term control of maize cell and root water permeability through plasma membrane aquaporin isoforms. *Plant, Cell and Environment* **35**:185–198.

Henzler T, Waterhouse RN, Smyth AJ, Carvajal M, Cooke DT, Schäffner AR, Steudle E, Clarkson DT. 1999. Diurnal variations in hydraulic conductivity and root pressure can be correlated with the expression of putative aquaporins in the roots of *Lotus japonicus*. *Planta* **210**:50–60.

Horie T, Kaneko T, Sugimoto G, Sasano S, Panda SK, Shibasaka M, Katsuhara M. 2011. Mechanisms of water transport mediated by PIP aquaporins and their regulation via phosphorylation events under salinity stress in barley roots. *Plant and Cell Physiology* **52**:663–675.

Horie T, Karahara I, Katsuhara M. 2012. Salinity tolerance mechanisms in glycophytes: an overview with the central focus on rice plants. *Rice* **5**:11.

Jang JY, Kim DG, Kim YO, Kim JS, Kang H. 2004. An expression analysis of a gene family encoding plasma membrane aquaporins in response to abiotic stresses in *Arabidopsis thaliana*. *Plant Molecular Biology* **54**:713–725.

Javot H, Maurel C. 2002. The role of aquaporins in root water uptake. *Annals of Botany* **90**:301–313.

Javot H, Lauvergeat V, Santoni V, Martin-Laurent F, Güçlü J, Vinh J, Heyes J, Franck KI, Schäffner AR, Bouchez D, Maurel C. 2003. Role of a single aquaporin isoform in root water uptake. *The Plant Cell* **15**:509–522.

Jozefkowicz C, Rosi P, Sigaut L, Soto G, Pietrasanta LI, Amodeo G, Alleva K. 2013. Loop A is critical for the functional interaction of two *Beta vulgaris* PIP aquaporins. *PLoS ONE* **8**:e57993.

Kaplan A, Gale J. 1974. Modification of the pressure-bomb technique for measurement of osmotic potential in halophytes. *Journal of Experimental Botany* **25**:663–668.

Karley AJ, White PJ. 2009. Moving cationic minerals to edible tissues: potassium, magnesium, calcium. *Current Opinion in Plant Biology* **12**:291–298.

Knipfer T, Fricke W. 2010. Root pressure and a solute reflection coefficient close to unity exclude a purely apoplastic pathway of radial water transport in barley (*Hordeum vulgare*). *New Phytologist* **187**:159–170.

Knipfer T, Fricke W. 2011. Water uptake by seminal and adventitious roots in relation to whole-plant water flow in barley (*Hordeum vulgare* L.). *Journal of Experimental Botany* **62**:717–733.

Knipfer T, Besse M, Verdeil JL, Fricke W. 2011. Aquaporin-facilitated water uptake in barley (*Hordeum vulgare* L.) roots. *Journal of Experimental Botany* **62**:4115–4126.

Krishnamurthy P, Ranathunge K, Nayak S, Schreiber L, Mathew MK. 2011. Root apoplastic barriers block Na^+ transport to shoots in rice (*Oryza sativa* L.). *Journal of Experimental Botany* **62**: 4215–4228.

Lindhauer MG, Haeder HE, Beringer H. 1990. Osmotic potentials and solute concentrations in sugar beet plants cultivated with varying potassium/sodium ratios. *Journal of Plant Nutrition and Soil Science* **153**:25–32.

Liu C, Li C, Liang D, Wei Z, Zhou S, Wang R, Ma F. 2012. Differential expression of ion transporters and aquaporins in leaves may contribute to different salt tolerance in *Malus* species. *Plant Physiology and Biochemistry* **58**:159–165.

Luu DT, Martinière A, Sorieul M, Runions J, Maurel C. 2012. Fluorescence recovery after photobleaching reveals high cycling dynamics of plasma membrane aquaporins in *Arabidopsis* roots under salt stress. *The Plant Journal* **69**:894–905.

Mahdieh M, Mostajeran A, Horie T, Katsuhara M. 2008. Drought stress alters water relations and expression of PIP-type aquaporin genes in *Nicotiana tabacum* plants. *Plant and Cell Physiology* **49**:801–813.

Martínez-Ballesta MC, Aparicio F, Pallás V, Martínez V, Carvajal M. 2003. Influence of saline stress on root hydraulic conductance and PIP expression in *Arabidopsis*. *Journal of Plant Physiology* **160**:689–697.

Maurel C. 1997. Aquaporins and water permeability of plant membranes. *Annual Review of Plant Physiology and Plant Molecular Biology* **48**:399–429.

Maurel C, Simonneau T, Sutka M. 2010. The significance of roots as hydraulic rheostats. *Journal of Experimental Botany* **61**:3191–3198.

Mittler R, Blumwald E. 2015. The roles of ROS and ABA in systemic acquired acclimation. *The Plant Cell* **27**:64–70.

Munns R, Tester M. 2008. Mechanisms of salinity tolerance. *Annual Review of Plant Biology* **59**:651–681.

Muries B, Faize M, Carvajal M, Martínez-Ballesta MC. 2011. Identification and differential induction of the expression of aquaporins by salinity in broccoli plants. *Molecular BioSystems* **7**:1322–1335.

Mutasa-Göttgens ES, Joshi A, Holmes HF, Hedden P, Göttgens B. 2012. A new RNASeq-based reference transcriptome for sugar beet and its application in transcriptome-scale analysis of vernalization and gibberellin responses. *BMC Genomics* **13**:99.

Niu X, Bressan RA, Hasegawa PM, Pardo JM. 1995. Ion homeostasis in NaCl stress environments. *Plant Physiology* **109**:735–742.

Pakniyat H, Armion M. 2007. Sodium and proline accumulation as osmoregulators in tolerance of sugar beet genotypes to salinity. *Pakistan Journal of Biological Sciences* **10**:4081–4086.

Peng YH, Zhu YF, Mao YQ, Wang SM, Su WA, Tang ZC. 2004. Alkali grass resists salt stress through high [K^+] and an endodermis barrier to Na^+. *Journal of Experimental Botany* **55**:939–949.

Postaire O, Tournaire-Roux C, Grondin A, Boursiac Y, Morillon R, Schäffner AR, Maurel C. 2010. A PIP1 aquaporin contributes to hydrostatic pressure-induced water transport in both the root and rosette of *Arabidopsis*. *Plant Physiology* **152**:1418–1430.

Qi X, Tai CY, Wasserman BP. 1995. Plasma membrane intrinsic proteins of *Beta vulgaris* L. *Plant Physiology* **108**:387–392.

Rahnama A, James RA, Poustini K, Munns R. 2010. Stomatal conductance as a screen for osmotic stress tolerance in durum wheat growing in saline soil. *Functional Plant Biology* **37**:255–263.

Reid KE, Olsson N, Schlosser J, Peng F, Lund ST. 2006. An optimized grapevine RNA isolation procedure and statistical determination of reference genes for real-time RT-PCR during berry development. *BMC Plant Biology* **6**:27.

Sack L, Holbrook NM. 2006. Leaf hydraulics. *Annual Review of Plant Biology* **57**:361–381.

Sade N, Moshelion M. 2014. The dynamic isohydric–anisohydric behavior of plants upon fruit development: taking a risk for the next generation. *Tree Physiology* **34**:1199–1202.

Schenk HJ, Espino S, Goedhart CM, Nordenstahl M, Cabrera HIM, Jones CS. 2008. Hydraulic integration and shrub growth form linked across continental aridity gradients. *Proceedings of the National Academy of Sciences of the USA* **105**:11248–11253.

Scholander PF, Hammel HT, Bradstreet ED, Hemmingsen EA. 1965. Sap pressure in vascular plants: negative hydrostatic pressure can be measured in plants. *Science* **148**:339–346.

Shabala S. 2013. Learning from halophytes: physiological basis and strategies to improve abiotic stress tolerance in crops. *Annals of Botany* **112**:1209–1221.

Shabala S, Cuin TA. 2008. Potassium transport and plant salt tolerance. *Physiologia Plantarum* **133**:651–669.

Shabala S, Shabala S, Cuin TA, Pang J, Percey W, Chen Z, Conn S, Eing C, Wegner LH. 2010. Xylem ionic relations and salinity tolerance in barley. *The Plant Journal* **61**:839–853.

Sharp RE, Poroyko V, Hejlek LG, Spollen WG, Springer GK, Bohnert HJ, Nguyen HT. 2004. Root growth maintenance during water deficits: physiology to functional genomics. *Journal of Experimental Botany* **55**:2343–2351.

Skorupa-Kłaput M, Szczepanek J, Kurnik K, Tretyn A, Tyburski J. 2015. The expression patterns of plasma membrane aquaporins in leaves of sugar beet and its halophyte relative, *Beta vulgaris* ssp. maritima, in response to salt stress. *Biologia* **70**:467–477.

Soto G, Fox R, Ayub N, Alleva K, Guaimas F, Erijman EJ, Mazzella A, Amodeo G, Muschietti J. 2010. TIP5;1 is an aquaporin specifically targeted to pollen mitochondria and is probably involved in nitrogen remobilization in *Arabidopsis thaliana*. *The Plant Journal* **64**:1038–1047.

Soto G, Stritzler M, Lisi C, Alleva K, Pagano ME, Ardila F, Mozzicafreddo M, Cuccioloni M, Angeletti M, Ayub ND. 2011. Acetoacetyl-CoA thiolase regulates the mevalonate pathway during abiotic stress adaptation. *Journal of Experimental Botany* **62**:5699–5711.

Steudle E. 2000. Water uptake by plant roots: an integration of views. *Plant and Soil* **226**:45–56.

Steudle E, Peterson CA. 1998. How does water get through roots? *Journal of Experimental Botany* **49**:775–788.

Suku S, Knipfer T, Fricke W. 2014. Do root hydraulic properties change during the early vegetative stage of plant development in barley (*Hordeum vulgare*)? *Annals of Botany* **113**:385–402.

Sutka M, Li G, Boudet J, Boursiac Y, Doumas P, Maurel C. 2011. Natural variation of root hydraulics in *Arabidopsis* grown in normal and salt-stressed conditions. *Plant Physiology* **155**:1264–1276.

Takase T, Ishikawa H, Murakami H, Kikuchi J, Sato-Nara K, Suzuki H. 2011. The circadian clock modulates water dynamics and aquaporin expression in *Arabidopsis* roots. *Plant and Cell Physiology* **52**:373–383.

Tardieu F, Davies WJ. 1993. Integration of hydraulic and chemical signaling in the control of stomatal conductance and water status of droughted plants. *Plant, Cell and Environment* **16**:341–349.

Tester M, Davenport R. 2003. Na^+ tolerance and Na^+ transport in higher plants. *Annals of Botany* **91**:503–527.

Turner NC. 1981. Techniques and experimental approaches for the measurement of plant water status. *Plant and Soil* **58**:339–366.

Tyerman SD, Niemietz CM, Bramley H. 2002. Plant aquaporins: multifunctional water and solute channels with expanding roles. *Plant, Cell and Environment* **25**:173–194.

Tyree MT. 2003. Hydraulic properties of roots. In: Visser EJW, De Kroon H, eds. *Root ecology*. Berlin: Springer, 125–150.

Vandeleur RK, Mayo G, Shelden MC, Gilliham M, Kaiser BN, Tyerman SD. 2009. The role of plasma membrane intrinsic protein aquaporins in water transport through roots: diurnal and drought stress responses reveal different strategies between isohydric and anisohydric cultivars of grapevine. *Plant Physiology* **149**: 445–460.

Vandeleur RK, Sullivan W, Athman A, Jordans C, Gilliham M, Kaiser BN, Tyerman SD. 2014. Rapid shoot-to-root signalling regulates root hydraulic conductance via aquaporins. *Plant, Cell and Environment* **37**:520–538.

Van den Honert TH. 1948. Water transport in plants as a catenary process. *Discussions of the Faraday Society* **3**:146–153.

Wan H, Zhao Z, Qian C, Sui Y, Malik AA, Chen J. 2010. Selection of appropriate reference genes for gene expression studies by quantitative real-time polymerase chain reaction in cucumber. *Analytical Biochemistry* **399**:257–261.

Wang W, Yang X, Zhang S, Sun Y. 2013. The root cortex cell hydraulic conductivity is enhanced with increasing chromosome ploidy in wheat. *Plant Physiology and Biochemistry* **68**:37–43.

Weatherley PE. 1950. Studies in the water relations of the cotton plant. I. The field measurement of water deficits in leaves. *New Phytologist* **49**:81–97.

